

Single-pulse Raman and photoacoustic spectroscopy studies of triaminotrinitrobenzene (TATB) and related compounds

W. M. Trott, A. M. Renlund, and R. G. Jungst

SAND--84-1974C

Sandia National Laboratories
Albuquerque, New Mexico 87185

DE85 010072

Abstract

Pulsed-laser-excited Raman scattering methods and photoacoustic spectroscopy have been applied to the study of porous, granular samples (i.e., pressed pellets) of 1,3,5-trinitrobenzene (TNB), 1-amino-2,4,6-trinitrobenzene (MATB), 1,3-diamino-2,4,6-trinitrobenzene (DATB) and 1,3,5-triamino-2,4,6-trinitrobenzene (TATB). Single-pulse spontaneous Raman spectra have been obtained for all four materials. Using 532-nm excitation, the intensity of the background emission observed with the Raman scattered light varies as TNB > MATB > DATB > TATB. This trend is compared to information on the long-wavelength absorption edge of MATB, DATB and TATB as determined by the photoacoustic spectra of these materials. Stimulated Raman scattering has been observed for three of the compounds with conversion efficiency as follows: DATB > TATB > MATB. In the case of TATB, this process may be limited by photo-induced chemical reactions. The relatively efficient formation of one or more stable photolysis products in TATB is evident on the basis of its photoacoustic spectrum. Preliminary single-pulse Raman scattering measurements on shocked TATB are also described.

Introduction

The development of predictive numerical models of initiation processes in heterogeneous (i.e., porous, granular) explosive materials would greatly benefit programs addressing issues of explosive safety, vulnerability and performance. The realization of this predictive capability requires much additional insight into the microscopic physical and chemical properties of heterogeneous explosive materials including the detailed response of these materials to shock compression. In this paper, we discuss the application of pulsed-laser-excited Raman scattering techniques and photoacoustic spectroscopy to the study of porous, granular samples of 1,3,5-triamino-2,4,6-trinitrobenzene (TATB) and related explosive compounds. This work is part of the effort we have undertaken to develop spectroscopic methods which are applicable to a wide variety of polycrystalline explosive materials including photosensitive samples (e.g., TATB) as well as shocked or detonating samples.¹⁻⁴

We have previously shown² that single-pulse spontaneous Raman spectra can be obtained from many unshocked heterogeneous explosives and that similar Raman scattering measurements can be made in the severe environment of a detonation. In addition, we reported the observation of intense, stimulated Raman scattering from TATB at the 1170 cm⁻¹ transition (ν_{NO_2}). The present work focuses on a series of nitroaromatic explosives including 1,3,5-trinitrobenzene (TNB), 1-amino-2,4,6-trinitrobenzene (MATB), 1,3-diamino-2,4,6-trinitrobenzene (DATB) and TATB. Single-pulse Raman spectra are shown and the results compared to conventional Raman studies where possible. Using 532-nm (frequency-doubled Nd:YAG laser) excitation, a background emission signal is observed in addition to the Raman scattered light. The intensity of this broadband emission varies as TNB > MATB > DATB > TATB. These results are compared to the corresponding photoacoustic spectra which are sensitive to weak absorption features near the excitation wavelength and show a blue-shifting of the long-wavelength absorption edge in the case of TATB. At sufficiently high laser intensities, stimulated Raman scattering has been observed at the 1342 cm⁻¹ transition in MATB and at the 831 cm⁻¹ and 1213 cm⁻¹ transitions in DATB as well as at the 1170 cm⁻¹ transition in TATB. The observed conversion efficiency follows the trend DATB > TATB > MATB. This trend is discussed in relation to the photoacoustic spectrum of TATB which demonstrates the efficient formation of one or more stable photolysis products upon exposure of the sample to light near 400 nm. Finally, we describe preliminary single-pulse Raman scattering results on shocked TATB.

Experimental

A discussion of the experimental design for the single-pulse Raman scattering studies has been presented elsewhere.² The essential details of the experimental arrangement are shown in Figure 1. Briefly, the 532-nm output of a frequency-doubled, pulsed Nd:YAG laser (~ 10 nsec FWHM) was mildly focused to a 1-mm-diameter circular spot on the surface of an explosive pellet. The laser energy reaching the sample was controlled by varying the time delay to the Q-switch. Maximum available energy at the sample was about 60 mJ. Each

JW

DISCLAIMER

This report was prepared as an account of work sponsored by an agency of the United States Government. Neither the United States Government nor any agency Thereof, nor any of their employees, makes any warranty, express or implied, or assumes any legal liability or responsibility for the accuracy, completeness, or usefulness of any information, apparatus, product, or process disclosed, or represents that its use would not infringe privately owned rights. Reference herein to any specific commercial product, process, or service by trade name, trademark, manufacturer, or otherwise does not necessarily constitute or imply its endorsement, recommendation, or favoring by the United States Government or any agency thereof. The views and opinions of authors expressed herein do not necessarily state or reflect those of the United States Government or any agency thereof.

DISCLAIMER

Portions of this document may be illegible in electronic image products. Images are produced from the best available original document.

sample was tested in an evacuated (< 0.1 Torr) explosion chamber in order to prevent optical breakdown and to avoid complications from signals due to air. The frequency-shifted radiation ($\lambda > 535$ nm) scattered from the sample was largely separated from the 532-nm light using a dichroic mirror plus appropriate cutoff filters and focused onto the entrance slit of a spectrometer. The dispersed spectrum was viewed by an intensified diode array and the signal processed by an optical multichannel analyzer. A 100-nsec-wide gate to the detector avoided signal loss due to timing jitter and provided some discrimination against other sources of radiation (e.g., fluorescence). Single-shot spectra in the wavelength range 540-600 nm were obtained using a 0.33-m, Jarrel-Ash spectrometer. The relative wavelength-dependent response of this detection system has been determined by recording the spectrum of a quartz-halogen lamp whose irradiance at different wavelengths is known. A 0.85-m, Spex double monochromator was utilized for frequency and linewidth measurements at 1.5 cm^{-1} resolution. Operation of this device in the spectrographic mode allowed 4-nm-wide portions of a given spectrum to be viewed and recorded on a single shot. Temporal profiles of Raman scattered light and the 532-nm laser pulse were examined by recording the signals from appropriately filtered biplanar phototubes (Hamamatsu R1193U-01) using Tektronix 7104 oscilloscopes (with 7A29 plug-in amplifiers). The overall time constant of this phototube and oscilloscope combination was about 0.4 nsec.

Samples of the four high explosive materials used in the Raman studies were prepared from approximately 100 mg of loose powder pressed to $> 90\%$ of the crystal density. For Raman scattering measurements on unshocked material, each explosive pellet was mechanically held in a fixture providing for linear and angular alignment. For studies of shocked TATB, a similar alignment fixture held an exploding bridgewire detonator (Reynolds Industries, RP-2) in place and a 6.4-mm-diameter, 1.6-mm-thick TATB pellet plus a 1.6-mm-thick PMMA spacer were mounted on the detonator output face using a thin layer of fast-setting epoxy. The detonator leads were connected to a 2.5 kV fireset using high-voltage vacuum feedthroughs. The specified detonator function time at this operating voltage is 1.8 μsec with a standard deviation of less than 25 nsec. Digital delay generators were used to set the fireset trigger pulse in relation to the probe laser and detection system gate.

The photoacoustic spectrometer is shown schematically in Figure 2. The photon source was a 1000-watt xenon arc lamp equipped with a water filter. A variable-frequency light chopper was used to modulate the light at 100 Hz. Wavelength scanning was accomplished using a 0.25-m monochromator (Spex Minimate). A quartz plate was used to pick off a small portion of the light exiting the monochromator and send it to a reference pyroelectric detector. The 50-mg samples of loose powder were contained in a quartz cell (0.3 cm^3 internal volume) coupled to a condenser microphone. Lock-in amplifiers were used to detect the sample and reference signals and their ratio was displayed versus wavelength to generate the sample spectrum. The wavelength resolution was approximately 10 nm.

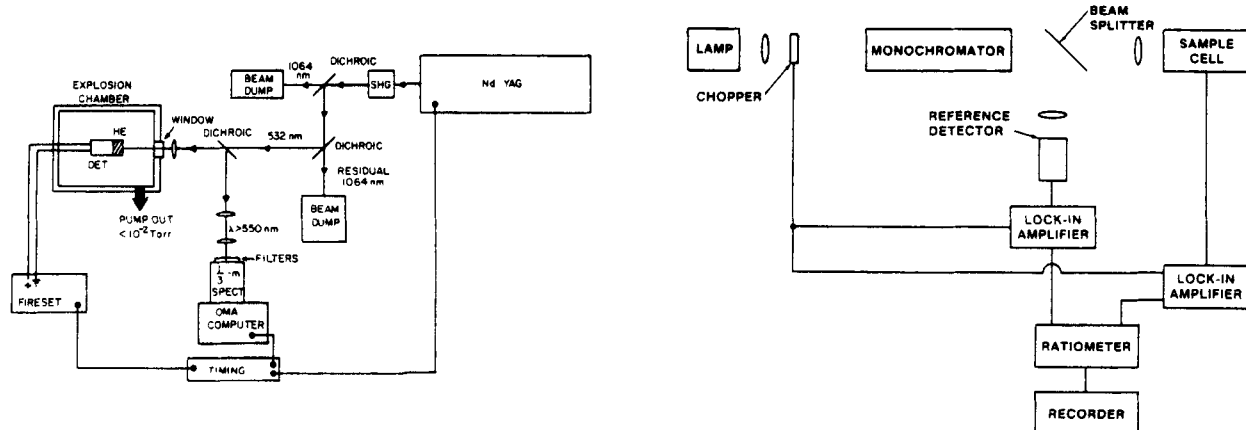


Figure 1. Schematic drawing of experimental design for pulsed-laser-excited Raman scattering measurements.

Figure 2. Schematic of photoacoustic spectrometer.

Results and discussion

Spontaneous Raman scattering and photoacoustic spectra

Raman spectra of unshocked TNB, MATB, DATB and TATB are shown in Figures 3, 4, 5 and 6, respectively. A single 532-nm laser pulse was used to generate each spectrum and the data are corrected for the wavelength-dependent response of the detection system. A different

laser energy was used for each sample in order to avoid nonlinear effects (see discussion below), as well as to provide a favorable ratio of Raman scattering to background emission. In Table I, observed band positions (determined with the higher resolution detection system) are listed and compared to results of cw laser Raman measurements, as available. The most intense peak in the spectrum of TNB occurs at 1366 cm^{-1} and has been previously assigned to the NO_2 symmetric stretching mode.⁵ This Raman shift falls within the characteristic range observed for symmetric NO_2 stretching vibrations in aromatic nitrocompounds.^{6,7} In contrast, the frequency observed for the intense peak due to the totally symmetric in-phase NO_2 stretch in TATB is much lower (1170 cm^{-1}). This substantial frequency perturbation has been attributed to extensive mixing of $-\text{NH}_2$ and $-\text{NO}_2$ group molecular motion among the fundamental modes of vibration due to a strong two-dimensional network of intra- and intermolecular hydrogen bonding in TATB.⁸ The observed positions of the dominant peaks in MATB and DATB (1342 cm^{-1} and 1213 cm^{-1} , respectively) indicate a consistent trend toward lower frequency corresponding to the extent of hydrogen bonding. The enhancement of the hydrogen bonding network and the attendant increase in overall molecular and lattice stability with increased amine substitution have been implicated as important factors in determining the shock initiation sensitivity of materials in this group.⁹

Figures 3-6 also show that the ratio of Raman scattering signal versus background emission improves in a consistent fashion with increased amine substitution. Comparison of the data on TNB and TATB with cw laser Raman studies highlights this trend. In terms of Raman signal discrimination against background, the pulsed-laser-excited Raman spectrum of

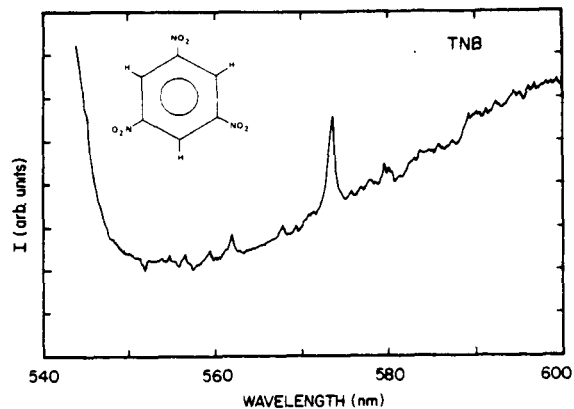


Figure 3. Single pulse Raman spectrum of 1,3,5-trinitrobenzene (TNB).

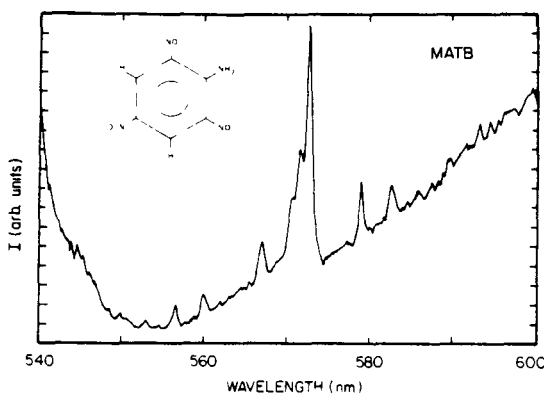


Figure 4. Single-Pulse Raman spectrum of 1-amino-2,4,6-trinitrobenzene (MATB).

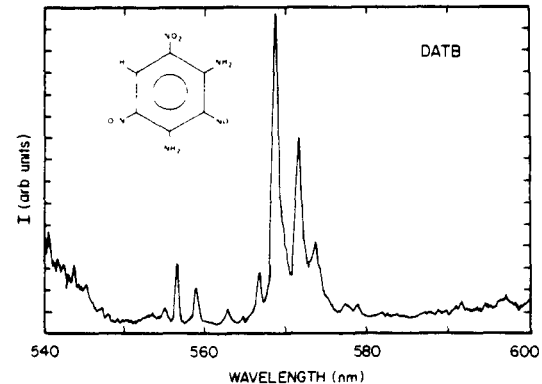


Figure 5. Single-pulse Raman spectrum of 1,3-diamino-2,4,6-trinitrobenzene (DATB).

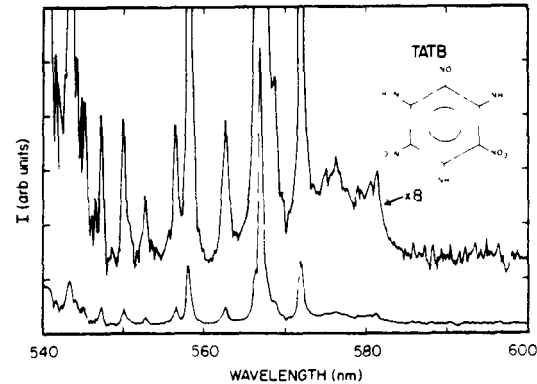


Figure 6. Single-pulse Raman spectrum of 1,3,5-triamino-2,4,6-trinitrobenzene (TATB).

TNB is inferior to the published results of Shurvell et al.⁵ In fact, many of the transitions identified by Shurvell et al. are not evident in the single-pulse Raman spectrum. On the other hand, Raman scattering obtained by pulsed-laser excitation appears to be very advantageous in the case of TATB. This material is known to be extremely photosensitive at ambient pressures and cw laser Raman studies produce high background scattering under these conditions.^{8,10,11} In this respect, the single-pulse Raman spectrum shown in Figure 6 is decidedly superior to the results of Deopura and Gupta¹⁰ and compares well with spectra recently obtained⁸ from TATB samples maintained at elevated pressures in order to suppress photolysis and thermal degradation.

Table I. Raman Frequencies (in cm^{-1}) for TNB, MATB, DATB, and TATB

<u>This work</u>	<u>cw laser Raman⁵</u>	<u>This work</u>	<u>This work</u>	<u>This work</u>	<u>cw laser Raman</u>
337	355	714	210	289	
371	370	818	357	367	
827	825	827	388	384	381 [10]
921	918	940	442	448	445 [10]
1003	1002	946	482	519	510 [10]
1185	1184	1092	512	539	
1299	1296	1166	674	612	606 [10]
1348	1345	1210	727	701	
1366	1365	1278	730	792	
1547	1547	1308	776	831	831 [8]
1624	1623	1342	831	879	880 [8]
3111	3100	1532	905	895	
		1630	1035	1029	1017 [10]
		3329	1151	1145	1147 [8]
			1160	1170	1170 [8]
			1213	1194	
			1314	1219	1229 [10]
			1363	1321	1303 [10]
			1487	1348	
			1526	1448	
			3288	1538	
				1606	
				3223	
				3324	

The observed variation of background emission intensity from pulsed-laser-excited TNB, MATB, DATB and TATB likely stems from differences in the absorption properties of these materials near 532 nm. To our knowledge, the electronic transitions associated with the weak absorption by these materials at this wavelength have not been characterized. Previous absorption studies of the corresponding solvated species have concentrated on prominent bands which occur at 420 nm or below; however, there is some evidence that MATB is a significantly stronger absorber at $\lambda > 440$ nm than DATB.¹² Depending on the exact nature of the absorption process, stronger emission from MATB might be expected if this relationship is maintained at 532 nm. In order to acquire additional information, we have examined samples of MATB, DATB and TATB using photoacoustic spectroscopy. In the present context, the advantages of this technique are its applicability to pure, granular materials and its apparent sensitivity to weak absorption features at $\lambda > 450$ nm. The spectra of the three materials are shown in Figure 7. The complex, nonlinear relationship between absorption cross section and the photoacoustic signal¹³ does not permit full interpretation of the data at 532 nm; however, there is ample evidence for substantial blue-shifting of the absorption edge in the case of TATB. This property may account for the relatively good quality of the single-pulse Raman spectrum for this molecule.

Another interesting feature of the TATB photoacoustic spectrum is the apparent weak absorption region near 675 nm. Further investigation has shown that this phenomenon is another manifestation of TATB's photosensitivity; one or more stable photoproducts are formed in the course of a normal wavelength scan. Scanning to higher wavelengths beginning at 550 nm produced no evident absorption feature whereas prolonged exposure of the TATB sample to 400-nm radiation resulted in significantly enhanced signal from 450-850 nm, as indicated in Figure 8. At least two new absorption bands were generated. In other work based on ESR measurements of uv-irradiated TATB extracted with dimethylsulfoxide, Britt et al. have suggested that an unusually stable free radical species occurs as a photoproduct.¹⁴ While this facile photolytic process clearly contributes to the high background scattering seen with conventional Raman methods, the pulsed-laser-excited TATB Raman spectrum obtained in this study is not similarly degraded. The photolysis apparently occurs on a time scale much longer than the ~ 10 -nsec laser pulse.

Stimulated Raman scattering

In an earlier paper, we reported intense nonlinear Raman scattering from porous, granular TATB at the 1170 cm^{-1} transition.² We identified this phenomenon as stimulated Raman scattering (SRS) on the basis of the following observations: (1) the near exponential dependence of scattering intensity as a function of laser energy, (2) the fact that the strongest spontaneous Raman line in the spectrum exhibits this growth, (3) occurrence of this phenomenon at different excitation wavelengths, (4) the definite correlation of the temporal profile of 1170 cm^{-1} scattering with intense mode spikes in

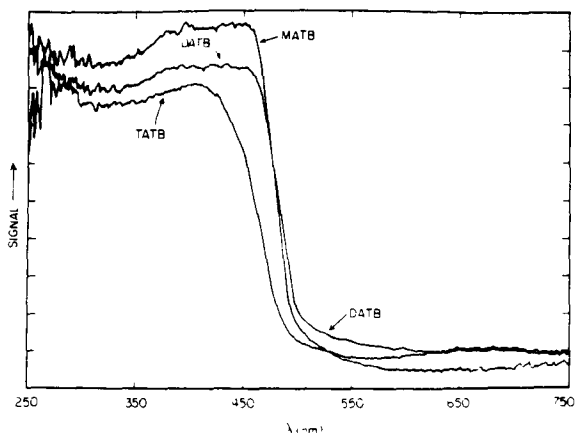


Figure 7. Photoacoustic spectra (250-750 nm) of MATB, DATB, and TATB.

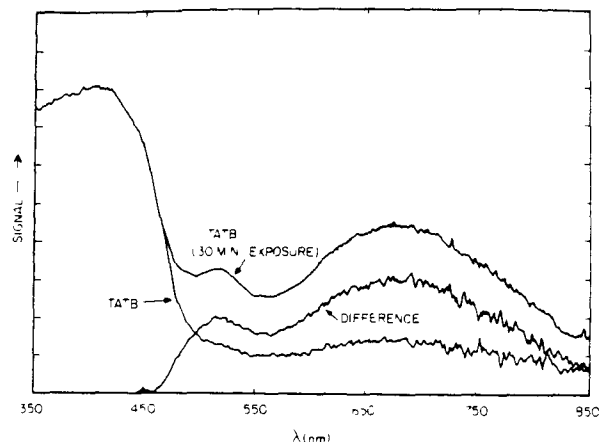


Figure 8. Photoacoustic spectrum of TATB with and without 30 minute exposure of the sample to 400-nm light. Difference signal indicates two distinct absorption bands.

the frequency-doubled Nd:YAG laser pulse and (5) narrowing of the 1170 cm^{-1} feature to a value near that of the pump laser bandwidth ($\sim 1.5\text{ cm}^{-1}$) at sufficiently high excitation energies. Data demonstrating the latter two effects are reproduced in Figures 9 and 10. Of the materials studied at that time, TATB was the only compound which exhibited SRS under our experimental conditions. Having extended our studies to different sample densities and various new materials, we have found that TATB is not unique in this regard. We report here SRS at the 1342 cm^{-1} transition in MATB and at two transitions (1213 cm^{-1} and 831 cm^{-1}) in the case of DATB. SRS from more than one vibrational mode in a given compound occurs infrequently.¹⁵ Transitions at 827 cm^{-1} in TNB and at 831 cm^{-1} and 879 cm^{-1} in TATB have been previously identified as NO_2 scissor modes^{5,8} and we attribute the 831 cm^{-1} line in DATB to a similar fundamental vibration. Hence, it is interesting that both modes exhibiting SRS in this compound are likely associated with the NO_2 moiety.

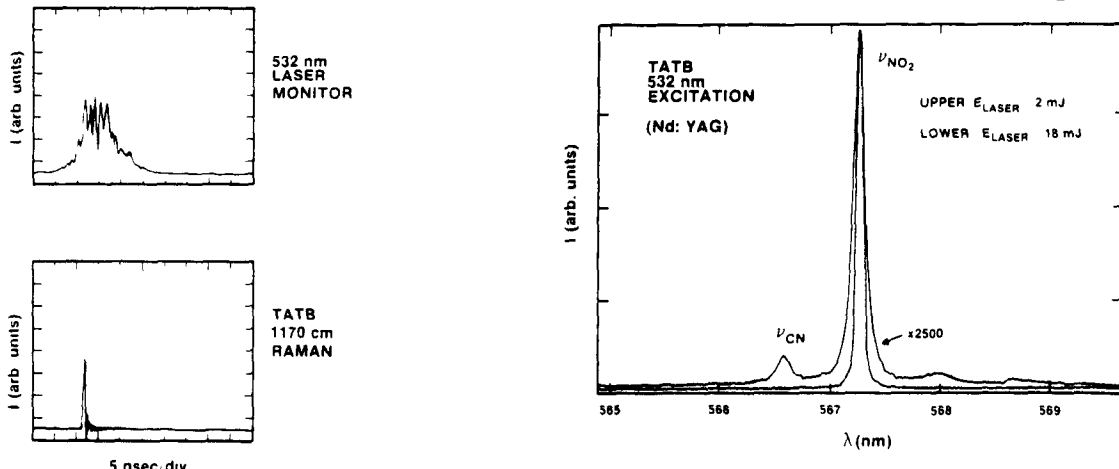


Figure 9. Simultaneously acquired temporal profiles of the frequency-doubled Nd:YAG laser pulse at 532 nm and the 567-nm (1170 cm^{-1} shifted) Raman signal from TATB. The Raman signal was isolated by a long-wave-pass filter (Schott OG-550) plus a narrowband interference filter (570 nm center wavelength; 10 nm width, FWHM).

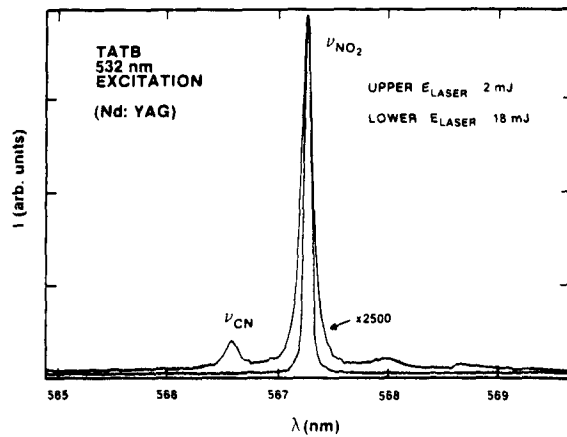


Figure 10. Single-pulse Raman spectra from TATB in the region of the intense 1170 cm^{-1} transition. Peak intensities have been normalized to illustrate narrowing of the Raman line width at higher excitation energy.

Figure 11 contains data showing the dependence of Raman scattering intensity on 532-nm laser energy for the 1342 cm^{-1} line in MATB, the 1213 cm^{-1} line in DATB and the 1170 cm^{-1} line in TATB. Although there is considerable scatter in the data due to shot-to-shot variations in the temporal mode structure of the excitation source (cf. Figure 9),

nonlinear growth of signal occurs in reasonably well-defined regions for each material with conversion efficiency varying as DATB > TATB > MATB. At sufficiently high laser energies, conversion into the second Stokes component near 2400 cm^{-1} has been observed in the case of DATB. Since we have not observed SRS at all from TNB, it would appear that increased amine substitution generally facilitates SRS in this class of compounds. Low thresholds for SRS are frequently observed at narrow lines associated with totally symmetric vibrations, as we see here.¹⁵ Table II lists estimated spontaneous Raman line widths for the various transitions exhibiting SRS plus the 1366 cm^{-1} feature in TNB. The value for the 1170 cm^{-1} peak in TATB agrees with the data of Satija and Swanson.⁸ With the exception of the 1213 cm^{-1} transition in DATB, the trend toward narrower line widths with increased amine substitution is consistent with the observed conversion efficiencies.

Table II. Estimated Spontaneous Raman Line Widths for the Transitions Exhibiting SRS in MATB, DATB, and TATB and for the Most Intense Transition in TNB.

Molecule (transition)	Line Width (in cm^{-1}) ^a
TNB (1366 cm^{-1})	8
MATB (1342 cm^{-1})	7
DATB (831 cm^{-1})	4
DATB (1213 cm^{-1})	19
TATB (1170 cm^{-1})	3

^aCalculated by assuming that the probe laser line width, instrumental line width and the spontaneous Raman line width add in quadrature.

It is possible that the large apparent line width of the higher frequency DATB feature may be due in part to multiple unresolved transitions in this region. However, line width measurements at laser energies above the threshold for SRS in DATB and TATB do not support this interpretation; i.e., the DATB feature remains significantly broader. Thus, the reasons for the apparent "reversal" in conversion efficiency for DATB and TATB are not clear. The previously discussed photo-induced chemical reactions in TATB may play a role in limiting the SRS efficiency for this compound. While deleterious effects due to photochemistry are not evident in the pulsed-laser-excited spontaneous Raman spectrum of TATB, we routinely observe a drastic reduction in the 1170 cm^{-1} SRS signal intensity when a given region of the sample is irradiated a second time. A comparable SRS "gain spoiling" effect does not occur in DATB.

Single-pulse Raman scattering from shocked TATB

We have shown that single-pulse Raman scattering measurements can be made in the severe environment of a detonating heterogeneous explosive. Measurements of spontaneous Raman scattering from detonating PETN and HMX have been described elsewhere.²⁻⁴ The capability of generating intense SRS from a variety of interesting explosive compounds could prove to be another useful diagnostic option for studies in very luminous environments. We have briefly addressed this possibility in the examination of shocked TATB. Raman spectra from the free surface of the unshocked and shocked material are shown in Figures 12 and 13, respectively. The configuration of the detonator, spacer and TATB pellet is also illustrated in Figure 13. We did not attempt to measure the shock pressure in the TATB sample in this experiment; however, fast framing camera records of the event indicate significant luminosity in the region of the shock front. These records also confirm the calculated time of 900 nsec for shock propagation from the detonator output face to the free surface of the TATB. Accordingly, the Raman spectrum in Figure 13 was generated approximately 600 nsec after shock interaction with the surface. At this time, we observe low background emission, a fairly uniform attenuation of the spontaneous Raman lines (cf. noise levels in Figures 12 and 13) and a much more pronounced decrease in the

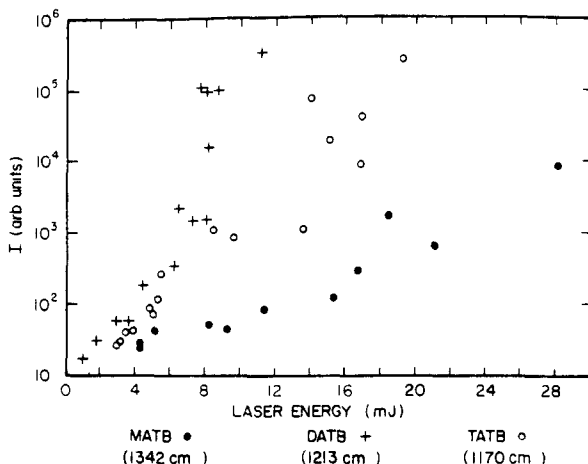


Figure 11. Laser energy dependence of Raman scattering for the 1342 cm^{-1} transition of MATB, the 1213 cm^{-1} transition of DATB and the 1170 cm^{-1} transition of TATB.

SRS intensity at 1170 cm^{-1} . In fact, the relative intensity of the 1170 cm^{-1} line in Figure 13 approaches that expected for spontaneous Raman scattering alone. This phenomenon does not necessarily indicate chemical modification, especially in view of the fact that Raman studies of TATB under static compression have provided no evidence of either pressure-induced chemistry or structural phase transformations up to pressures of 160 kbar at room temperature.⁸ The selective decrease of the 1170 cm^{-1} line may arise from a subtle structural modification or may simply reflect a significant density change. The latter possibility is suggested by the fact that we have observed a density effect on SRS intensity from different pressings of PETN (unshocked).¹⁶ More studies on shocked TATB are planned in order to characterize this phenomenon.

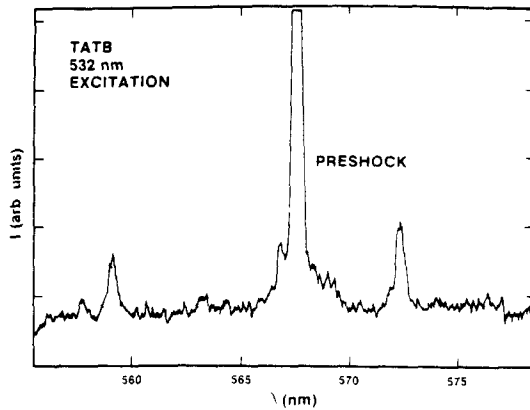


Figure 12. Single-pulse Raman spectrum of unshocked TATB showing transitions in the $800\text{-}1500\text{ cm}^{-1}$ region.

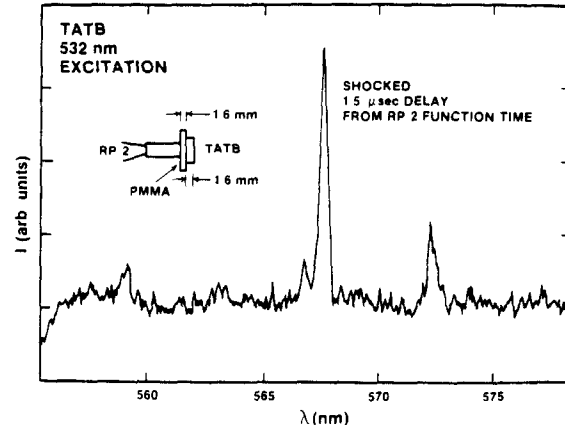


Figure 13. Single-pulse Raman spectrum of shocked TATB as recorded by the optical multichannel analyzer (100-nsec gate width). Laser energy was the same as for Figure 12.

Summary

As part of the effort we have undertaken to gain information on microscopic physical and chemical processes in the initiation and detonation of explosives, we have applied pulsed-laser-excited Raman techniques and photoacoustic spectroscopy to the study of porous, granular samples of TATB and related compounds. The Raman studies have shown that single-pulse techniques are applicable to some photosensitive materials such as TATB and may also be utilized as a spectroscopic probe in shock and detonation experiments. The intensity of the broadband emission observed with spontaneous Raman scattering diminishes with increased amine substitution on trinitrobenzene. On the basis of the photoacoustic spectra of MATB, DATB and TATB as well as published results on the corresponding solvated species, we attribute this trend to diminished interference due to lower absorption coefficients for the higher substituted molecules near 532 nm. Stimulated Raman scattering is generally favored by increased amine substitution in this series of compounds; however, observed conversion efficiency is higher in DATB than in TATB. The SRS efficiency in the latter compound may be limited by competition from photo-induced chemical reactions. We have observed a relatively large decrease in the intensity of the 1170 cm^{-1} (SRS) line of TATB under shock conditions. Further experiments are planned in order to characterize this effect.

Acknowledgements

We gratefully acknowledge the fine technical assistance of H. C. Richardson and J. C. Pabst. This work was performed at Sandia National Laboratories, Albuquerque, New Mexico, supported by the U. S. Department of Energy under contract number DE-AC04-76DP00789.

References

1. Renlund, A. M., and Trott, W. M., "Spectra of Visible Emission from Detonating PETN and PBX 9407," SAND83-2168, Sandia National Laboratories, Albuquerque, NM, February 1984.
2. Trott, W. M., and Renlund, A. M., *Applied Optics* (in press).
3. Renlund, A. M., and Trott, W. M., "Spectroscopic Studies of Detonating Heterogeneous Explosives," *Proceedings, 10th Annual Technical Meeting on Physics of Explosives*, DEA-7304. M. F. Zimmer, ed. (in press).
4. Trott, W. M., and Renlund, A. M., "Time-Resolved Spectroscopic Studies of Detonating Heterogeneous Explosives," *Eighth Symposium (International) on Detonation*, Albuquerque, NM, July 1985 (submitted).

5. Shurvell, H. F., Norris, A. R., and Irish, D. E., Can J. Chem., Vol. 47, p. 2515. 1969.
6. Green, J. H. S., Kynaston, W., and Lindsey, A. S., Spectrochim. Acta, Vol. 17, p. 486. 1961.
7. Dollish, F. R., Fateley, W. G., and Bentley, F. F., Characteristic Raman Frequencies of Organic Compounds, Wiley, New York, 1974.
8. Satija, S. K., and Swanson, B. I., unpublished data.
9. Rogers, J. W., Jr., Peebles, H. C., Rye, R. R., Houston, J. E., and Binkley, J. S., J. Chem. Phys., Vol. 80, p. 4513. 1984.
10. Deopura, B. L., and Gupta, V. D., J. Chem. Phys., Vol. 54, p. 4013. 1971.
11. Towns, T. G., Spectrochim. Acta, Vol. 39A, p. 801. 1983.
12. Minesinger, R. R., and Kamlet, M. J., J. Am. Chem. Soc., Vol. 91, p. 4155. 1969.
13. Rosencwaig, A., Photoacoustics and Photoacoustic Spectroscopy, Wiley, New York, 1980. pp. 93-124.
14. Britt, A. D., Moniz, W. B., Chingas, G. C., Moore, D. W., Heller, C. A., Ko, C. L., Propellants and Explosives, Vol. 6, p. 94. 1981.
15. Eckhardt, G., IEEE J. Quantum Electron., Vol. 2, p. 1. 1966.
16. Trott, W. M., and Renlund, A. M., unpublished data.

DISCLAIMER

This report was prepared as an account of work sponsored by an agency of the United States Government. Neither the United States Government nor any agency thereof, nor any of their employees, makes any warranty, express or implied, or assumes any legal liability or responsibility for the accuracy, completeness, or usefulness of any information, apparatus, product, or process disclosed, or represents that its use would not infringe privately owned rights. Reference herein to any specific commercial product, process, or service by trade name, trademark, manufacturer, or otherwise does not necessarily constitute or imply its endorsement, recommendation, or favoring by the United States Government or any agency thereof. The views and opinions of authors expressed herein do not necessarily state or reflect those of the United States Government or any agency thereof.